

# Compact readout system for chipless passive LC tags and its application for humidity monitoring

P. Escobedo<sup>1</sup>, A. Martínez-Olmos<sup>1</sup>, J. Fernández-Salmerón<sup>2</sup>, A. Rivadeneyra<sup>2</sup>, L.F. Capitan-Vallvey<sup>3</sup>, A.J. Palma<sup>1</sup>, M.A. Carvajal<sup>1,\*</sup>,

Address:

<sup>1</sup> ECsens, CITIC-UGR, Departamento de Electrónica y Tecnología de Computadores. Universidad de Granada, E-18071 Granada, Spain.

<sup>2</sup> Institute for Nanoelectronics, Technical University of Munich, Theresienstr. 90, DE-80333, Munich, Germany.

<sup>3</sup> ECsens, Facultad de Ciencias, Departamento de Química Analítica. Universidad de Granada, E-18071 Granada, Spain.

mail: [carvajal@ugr.es](mailto:carvajal@ugr.es)

## Abstract

The development of a contactless readout system for High Frequency (HF) tags and its application to relative humidity monitoring is presented. The system consists of a Colpitts oscillator circuit whose frequency response is determined by a built-in logic counter of a microcontroller unit. The novel readout strategy is based on the frequency response change due to the inductive coupling between the coil of the Colpitts oscillator and the load impedance of a parallel LC resonator tag, as a result of the variation of the humidity sensing capacitor. The frequency is monitored with a low cost microcontroller, resulting in a simple readout circuit. This passive LC tag has been directly screen-printed on a humidity-sensitive flexible substrate. ~~The readout circuit exploits the tag resonance frequency shift due to the change of the printed capacitive sensor as a function of humidity.~~ The readout circuit experimental uncertainty as frequency meter was 0.72 kHz in the HF band. A linear temperature drift of  $(-1.52 \pm 0.17)$  kHz/°C was obtained, which can be used to apply thermal compensation if required. The readout system has been validated as a proof of concept for humidity measurement, obtaining a significant change of about 260 kHz in the resonance frequency of the Colpitts oscillator when relative humidity varies from 10% to 90%, with a maximum uncertainty of  $\pm 3\%$ . Therefore, the proposed readout system stands as a compact, low-cost, contactless solution for chipless HF tags that avoids the use of bulky and costly equipment for the analog reading of wireless passive LC sensors.

**Keywords:** Readout system, Passive LC tag, Chipless, Inductive coupling, Colpitts oscillator.

## 1. Introduction

The compatibility of Printed Electronics (PE) and sensors with flexible substrates has enabled the development of sensor systems in attractive form factors than can be deployed, for instance, into pharmaceutical or intelligent food packaging applications [1–3]. Among the different parameters of interest, the monitoring and control of humidity has been employed in different industrial applications such as smart packaging of goods and food to ensure quality preservation [4–7] or humidity surveillance within construction structures [8,9] among others. LC wireless passive sensors are a suitable solution in applications where powered and wired sensors are not possible [10–13].

The transduction mechanism of humidity capacitive sensors requires the use of materials whose electrical permittivity changes accordingly to the environmental relative humidity [14]. Several strategies have been followed to achieve this sensing capability, such as the deposition of a sensing layer over capacitive patterns [15–17] or the use of humidity-sensitive substrates [18–20]. For instance, a paper-based moisture sensor that uses the hygroscopic character of paper to measure patterns and rate of respiration was reported [21]. The most common planar capacitor design is the interdigitated electrode structure (IDE) [7,10,14–16], although others have been proposed such as a serpentine electrode structure (SRE) [18,22].

The inclusion of sensing capabilities into Radiofrequency Identification (RFID) tags brings added value to this contactless, non-line-of-sight identification and data transmission technology [23,24]. When the RFID tag is used as an electromagnetic sensor, different changes in the analog response of the tag have been associated to a variation of the sensed magnitude. This approach has been used to develop humidity sensors in flexible High Frequency (HF) tags by exploiting the RFID tag resonance frequency shift measurement. Polyimide, a material sensitive to moisture, was employed as substrate of a printed inductor and an interdigitated capacitor (using screen and inkjet printing techniques) to form an LC resonator for moisture detection [18]. The same operating principle was used for Ultra-High Frequency (UHF) tags [25]. Moreover, a passive RFID gas sensor with a resonant antenna coated with a gas-sensing film and an IC memory chip was presented [26]. A chipless RFID tag consisting of two inkjet-printed planar LC resonators was developed for humidity detection utilizing paper substrate as sensing material [20]. Another example to measure threshold humidity in a UHF tag by changing the antenna input impedance was proposed [27]. Very recently, a flexible RFID tag for humidity and temperature sensing has been proposed [28]. In this chipless tag, the variations of the monitored magnitudes are associated to changes in the measured level of the backscattered power. Mraović et al. proposed a screen-printed capacitive humidity sensor integrated in a UHF tag and fabricated on recycled paper and cardboard for smart packaging applications [29]. Other examples of flexible RFID tags as electromagnetic sensors can be found in literature for moisture sensing [30–32]. There are some other high stable quartz methods using capacitive sensor with low value (a few pF) also for humidity measurement, which explain how to compensate environment effect [33–36].

Among the different solutions, chipless approach is a very promising one to actually achieve a cost-effective transfer of fully printed sensing tags to industrial manufacturing processes [20,37]. Nevertheless, costly and bulky equipment such as impedance analyzers

[4,8,18], spectrum analyzers [38] or vector network analyzers (VNAs) [20,28] are mostly required to read the sensed magnitude based on analog measurements such as impedance or frequency spectra. Zhang et al. [39] developed an ad-hoc system to measure the relative humidity using a resonant LC tag, monitoring the real part of the readout coil impedance.

To overcome this shortcoming, here we present the development of a low-cost, portable, non-contact LC readout circuit for sensing-enabled HF RFID tags and its application to relative humidity monitoring. The reader circuit is based on capacitive sensing by means of a Colpitts oscillator. The ambient humidity modifies the oscillation frequency of the Colpitts by the capacitive load change of an inductively coupled humidity-sensitive LC tag. The frequency of the oscillator is registered by a microcontroller. The main advantage of this technique is the very simple electronic readout circuit as it will be shown later. The LC tag consists of a screen-printed chipless passive system based on a parallel LC resonator structure. In the literature, there are a few examples of capacitive sensors with Colpitts oscillator for heartbeat, respiration activity and position monitoring [40–45]. Works have been also published on inductively coupled passive resonance sensors [13,39,46–49].

## 2. Materials and methods

The readout circuit was fabricated on FR4 substrate with 35  $\mu\text{m}$  thick copper using a mechanical milling machine model ProtoMat<sup>®</sup> S100 (LPKF Laser & Electronics AG, Garbsen, Germany). The complete LC tag (loop inductor and capacitor) was screen-printed using a Serfix III screen printing machine (Seglevint SL, Barcelona, Spain) on 75  $\mu\text{m}$  thick flexible Polyimide Kapton<sup>®</sup> HN substrate (DuPont<sup>™</sup>, Wilmington, DE, USA). The screen mesh used for printing consisted of an aluminum rectangular structure of 50 cm  $\times$  35 cm with mesh density of 120 Nylon threads per centimeter (T/cm) allowing a minimum width pattern of 300  $\mu\text{m}$ . The patterns were printed using the conductive silver-based ink SunTronic CRSN 2442 (Sun Chemical, New Jersey, USA). After printing, a thermal sintering process was carried out at 120  $^{\circ}\text{C}$  during 20 minutes in a convection air oven Venticell VC55 (MMM Medcenter Einrichtungen GmbH, Munich, Germany). Finally, a bridge line was attached to close the circuit using the conductive resin Epoxy EPO-TEK<sup>®</sup> H20E (Epoxy Technology Inc., Billerica, USA). The Epoxy resin was cured in the oven at 150  $^{\circ}\text{C}$  for 15 minutes.

Physical dimensions of the LC tag components were optimized via numerical simulation using Advanced Design System (ADS) simulator (Keysight Technologies, Santa Clara, CA, USA) and COMSOL Multiphysics<sup>®</sup> (Comsol Inc., Burlington, MA, USA). The design goal was to achieve the minimum possible dimensions accounting for the limitations of the printed technology. Impedance frequency characterization of the reader and tag systems and their components (inductors and capacitors) separately was carried out using an Agilent 4294A Precision Impedance Analyzer and a 42941A impedance probe kit (Keysight Technologies, Santa Clara, CA, USA). Readout system calibration as frequency meter was performed with an Infiniium MSO9104A oscilloscope (Keysight Technologies, CA, USA).

The stationary thermal drift measurements of the readout system and the humidity calibration of the full system (LC tag and readout system) were controlled in a climatic chamber VCL4006

(Vötsch Industrieteknik, Germany) along with an external compressed air dryer from the same manufacturer to extend relative humidity range from 10 % to 98 % within a temperature range from 10 to 95 °C. According to the technical data provided by the manufacturer, this climate chamber model has a humidity deviation in time from  $\pm 1$  to  $\pm 3$  % and a temperature deviation in time from  $\pm 0.3$  to  $\pm 0.5$ °C relative to the set value.

### 3. Detection principle of the readout circuit

The resonance frequency of a Colpitts oscillator circuit,  $f_{osc}$ , is given by [50]:

$$f_{osc} = \frac{1}{2\pi\sqrt{L_{osc}C_{osc}}} \quad (1)$$

where  $L_{osc}$  is the total inductance of the oscillator coil and  $C_{osc}$  is the total capacitance of the circuit in parallel to the oscillator coil. The readout technique proposed here is based on the inductive coupling between the Colpitts oscillator coil and the printed LC tag coil, which contains a sensing-enabled capacitance (see Figure 1a). As we will show below, a contactless way to measure capacitances is used in this study. It must be taken into consideration that the coupled system must operate in the inductive region of the LC tag impedance to ensure an inductive coupling.

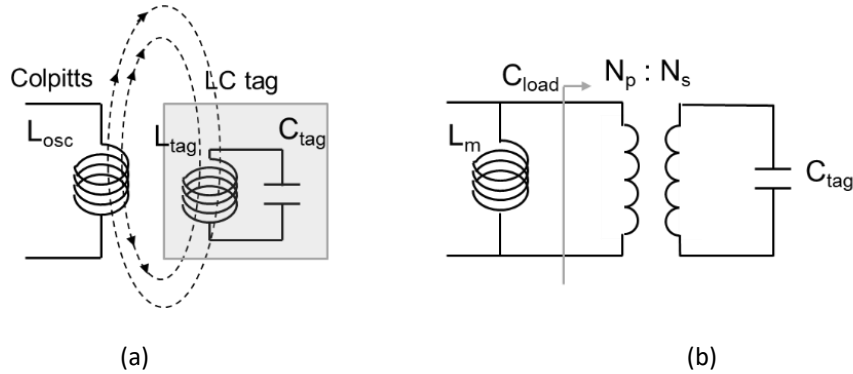


**Figure 1.** (a) Inductive coupling between the oscillator and the tag coils, (b) Ideal transformer model of this inductive coupling where  $L_m$  corresponds to magnetizing inductance of the readout coil [51].

When both coils are inductively coupled, it can be modelled as a transformer with air core. Therefore, the secondary impedance can be determined by measuring the impedance at the primary winding. If the transformer is considered as ideal, the contribution to the capacitance at the primary winding (in the readout circuit),  $C_{load}$ , due to the tag capacitor,  $C_{tag}$  is given by:

$$C_{load} = \left(\frac{N_s}{N_p}\right)^2 C_{tag}, \quad (2)$$

where  $N_s$  and  $N_p$  represent the turn number of secondary and primary windings respectively of the transformer model (Figure 1b). This capacitive load is in parallel with the capacitance of the uncoupled Colpitts oscillator,  $C_{osc}$ . Therefore, total loaded oscillator capacitance,  $C'_{osc}$  when the LC tag is inductively coupled can be approximately written as:

$$C'_{osc} = C_{osc} + C_{load} = C_{osc} + \left(\frac{N_{tag}}{N_{osc}}\right)^2 C_{tag}. \quad (3)$$

To account for the magnetic flux losses (coupling factor less than unity) [52], we consider that the actual load capacitance will be a fraction of  $C_{load}$ , in any case, keeping the additive dependence with  $C_{tag}$  shown in Equation 3. Because of the coupling, this increment of oscillator capacitance ( $C'_{osc} > C_{osc}$ ) will cause a reduction of the resonance frequency according to Equation 1. Thus, we are assuming that any change in the capacitive sensor  $C_{tag}$  will produce a  $f_{osc}$  shift. Therefore, the readout technique consists of registering changes in the oscillation frequency of the Colpitts circuit when the LC tag coil is inductively coupled to the Colpitts oscillator coil. The effect of inductive coupling on the reduction of the oscillator frequency will be very similar if the relative position of both coils is always the same, therefore it can be corrected using a calibration process, as the authors report in the present work.

#### 4. Readout circuit

The readout circuit is composed by a bipolar common-base Colpitts oscillator circuit and a frequency counter implemented in a microcontroller unit (MCU) as shown in Figure 2. The interface between them is buffered to minimize the load effect and to adapt the oscillator output level to the digital input. This digital signal is connected to the counter input of the MCU. Finally, the oscillation frequency is calculated from the registered pulses and sent to a personal computer via USB.

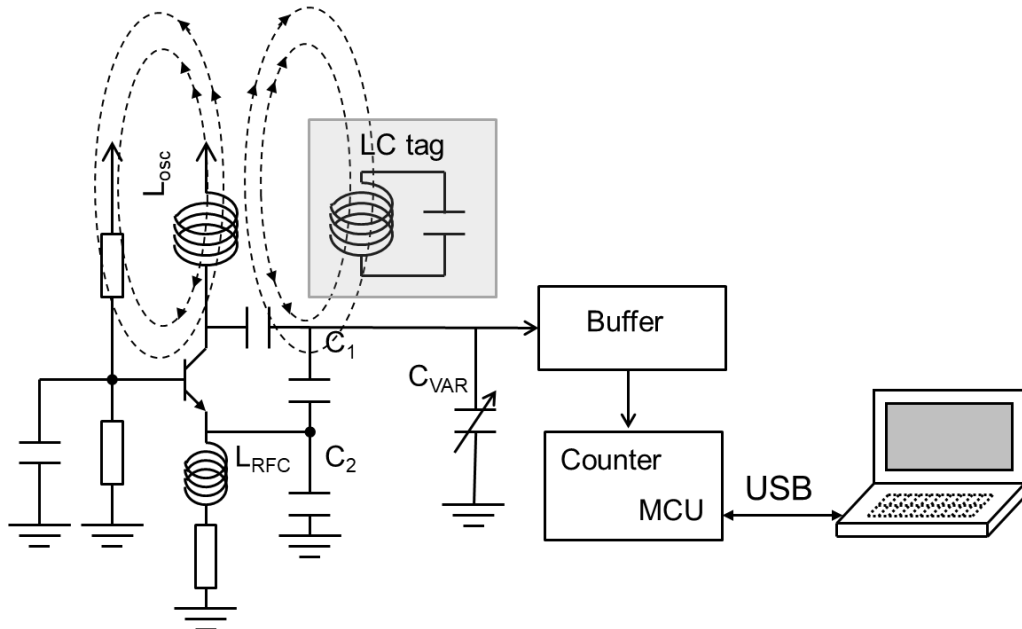


**Figure 2.** System schema of the reader system and the LC tag inductively coupled to the Colpitts oscillator coil.

The total oscillator capacitance without the LC tag,  $C_{osc}$ , is given by:

$$C_{osc} = \frac{C_1 C_2}{C_1 + C_2} + C_{VAR} \quad (4)$$

where  $C_1$  and  $C_2$  form the feedback capacitive voltage divider and  $C_{var}$  is a variable capacitor to tune accurately the resonance frequency. The HF frequency band (13.56 MHz) was used for compatibility with RFID tags.

The bipolar transistors BC547C (NXP Semiconductors, Eindhoven, The Netherlands) are used in the Colpitts and buffer circuits. The output of the oscillator is connected to the common-collector buffer for impedance decoupling. Counter pulses are registered during 25 ms as a compromise between speed and accuracy of the measurement and then, resonance frequency is computed within the microcontroller PIC18F2553 (Microchip, Palo Alto, USA). The buffered oscillator signal acts as a clock signal for one microcontroller timer (TIMER0), while another timer (TIMER1) controls the acquisition time. Accounting for the application developed in this work, a commercial relative humidity sensor, SHT15 (Sensirion, Stäfa, Zürich, Switzerland), was included in the reader unit for calibration purpose. A photograph of the prototyped readout unit is shown in Figure 3.

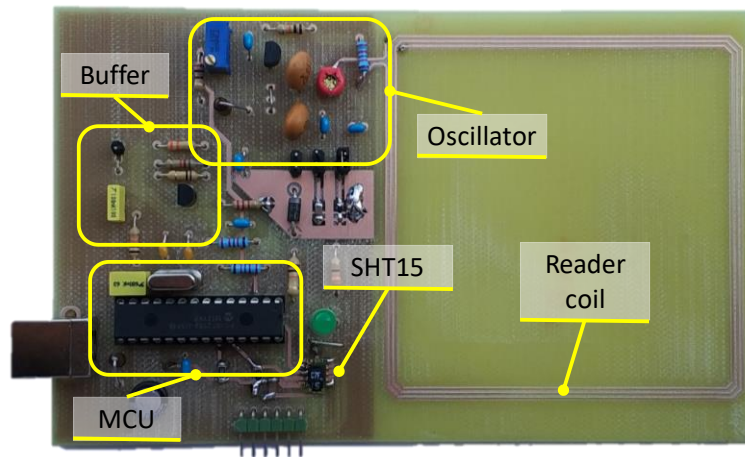


**Figure 3.** Image of the readout system showing the relevant components (Dimensions: 15×9×1.2 cm).

To achieve proper readout system operation, the oscillator must work at a frequency in the inductive region of the tag impedance to ensure inductive coupling, therefore it must be lower than 13.56 MHz. The oscillator inductor is a square coil targeting an inductance of 2.5  $\mu\text{H}$  by three square turns on an 8x8 cm<sup>2</sup> area. The central area is wide enough to locate the tag over it, avoiding overlapping between the reader and the tag coils (see Figure 3). In Figure 4, the L-Q spectra are displayed for the fabricated inductance of the readout unit where  $L_{osc} = 2.512 \pm 0.002 \mu\text{H}$  at 13.56 MHz with a quality factor of  $Q = 61.4 \pm 0.8$ . The measured self-resonance frequency was  $39.89 \pm 0.13$  MHz.

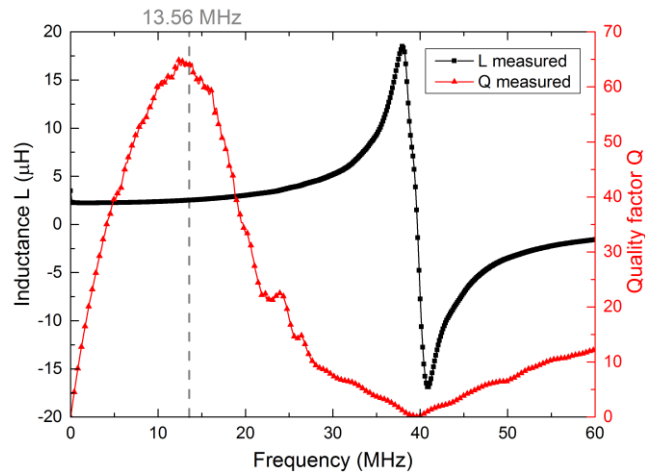


**Figure 4.** Measured frequency response of the reader coil.

With this reader coil, two ceramic capacitors of 56 pF were used as  $C_1$  and  $C_2$ , and a variable capacitor with a manual trimmer from 5 to 50 pF was included in parallel to tune the oscillation frequency thus, frequencies from 11.8 to 16.4 MHz could be settled.

The calibration of the frequency counter implemented in our readout system was carried out within the previous frequency range. To do so, we registered the pulses (frequency) provided by our readout circuit and the frequency measured by the oscilloscope. During the calibration, the probe of the oscilloscope was connected to the output of the buffer instead of to the oscillator output to avoid the load effect of the probe capacitance (11 pF). An excellent correlation ( $R^2=0.999$ ) was found between the oscilloscope and our reader measurements. The experimental uncertainty of the frequency counter was 0.72 kHz, measured as the standard deviation of the experimental data. This value represents the uncertainty in the determination of the Colpitts oscillation frequency and, consequently, in the magnitude determination when coupled to the LC sensing tag. Thermal drift of the oscillator circuit was also studied by placing the reader unit into the climate chamber and registering the oscillation frequency when temperature was increased from 10 °C to 50 °C. The calculated linear thermal coefficient was  $(-1.52 \pm 0.17)$  kHz/°C, which can be used to apply thermal compensation when required.

## 5. LC humidity sensing tag

Figure 5 shows the footprint, geometric dimensions and photographs of the screen printed LC tag, which basically consists of a planar loop inductor in parallel with an interdigitated (IDE) capacitor. In comparison with other structures, planar IDE capacitors allow more direct interaction with the surrounding environment and, consequently more sensitivity with the same area [16]. To simplify the fabrication process, we have directly used a polyimide flexible substrate as sensing element. The electrical permittivity of this substrate linearly increases with relative humidity of the environment due to the water absorption and the subsequent dielectric constant increment [53]. This variation with humidity produces changes in the capacitance of the printed LC tag. The IDE capacitance as a function of relative humidity has been fitted to a linear curve between 20 and 70% RH showing a higher slope above 70% RH [16,54,55]. Both trends can be jointly fitted to a quadratic polynomial curve.

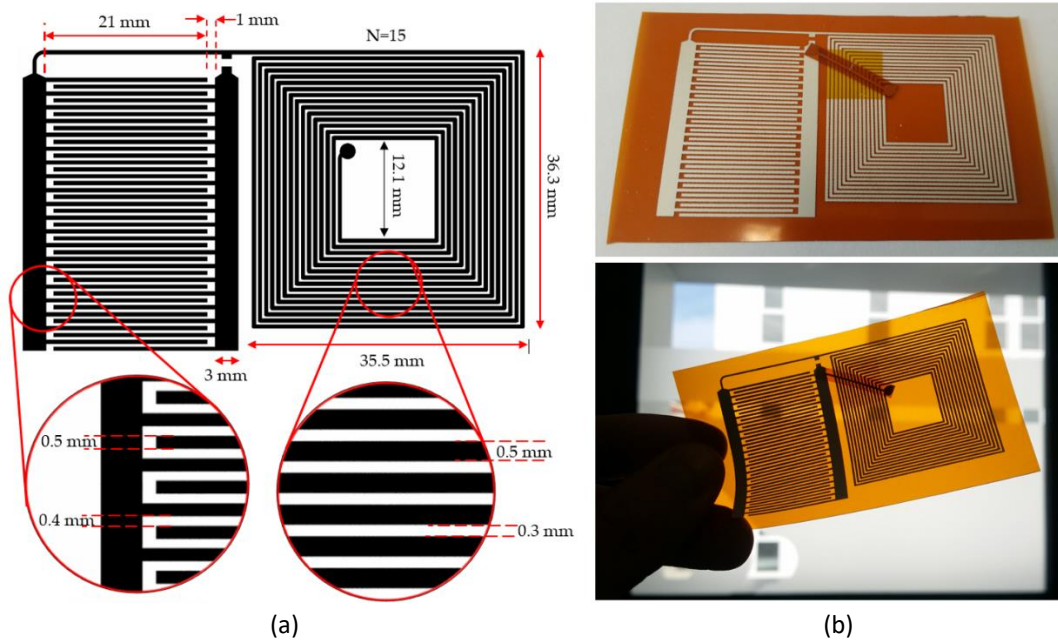
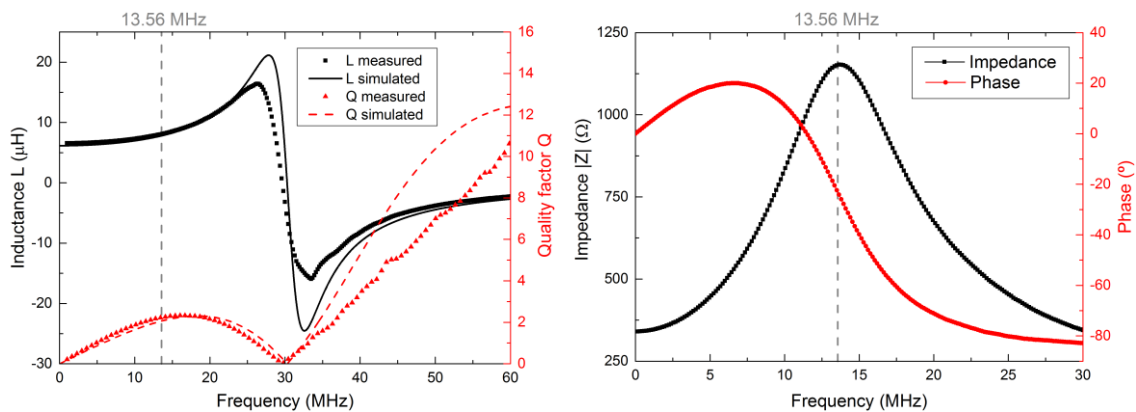


**Figure 5.** (a) Footprint and geometric dimensions of the LC tag and (b) photographs of the printed tag.

The tag was designed to resonate at approximately 13.56 MHz (HF band). In the case of the loop inductor, a simulated value of  $7.8 \mu\text{H}$  with a quality factor of 2.06 was obtained at 13.56 MHz (see Figure 6a). A capacitance of 3 pF in parallel with the inductor was included in the simulation to account for the probe parasitic capacitance. For the IDE capacitive structure, a simulated value of 18 pF was calculated at 13.56 MHz.

A set of five individual planar inductors and capacitors were fabricated and electrically characterized. The average measured for the inductors value was  $7.88 \pm 0.09 \mu\text{H}$  at 13.56 MHz with an average quality factor of  $2.11 \pm 0.12$ , as shown in Figure 6a. As for the capacitors, an average capacity value of  $18.6 \pm 0.4 \text{ pF}$  was obtained at the same frequency. Both values are in very good agreement with the simulated ones. The humidity response of this type of screen-printed IDE capacitors was evaluated in previous works [22,56]. After this, the tag was fabricated and the AC electrical characterization of the complete tag was performed by measuring its impedance, both magnitude and phase. As depicted in Figure 6b, the resonance frequency of the LC tag was measured at  $13.61 \pm 0.05 \text{ MHz}$  in dry atmosphere, very close to the targeted resonant frequency of 13.56 MHz.



(a)

(b)

**Figure 6.** (a) Simulated and measured frequency response of the planar inductor. (b) Measured impedance and phase of the parallel LC circuit.

The stationary humidity conditions of the LC tag were controlled in the climatic chamber at constant temperature (20°C). Relative humidity inside the climate chamber was varied from 10 to 90%. Three set of measurements were taken for each relative humidity to obtain a representative average value. Humidity inside the climate chamber was measured using the SHT15 sensor included in the readout unit, which has a typical accuracy of  $\pm 2.0$  %RH. The readout distance was fixed at 1 cm to ensure good coupling while maintaining the same conditions for all the measurements. The obtained results showed a resonance frequency shift of the Colpitts oscillator circuit from 12.30 MHz at 10% RH to 12.04 MHz when RH is increased up to 90%. Therefore, there was a significant change of about 260 kHz in the resonance frequency of the Colpitts oscillator circuit. Considering Equation 1 and 3 and assuming a quadratic behavior of the  $C_{tag}$  with the relative humidity (RH), the expected theoretical relationship is given by:

$$f_{osc}(RH) = \frac{1}{2\pi\sqrt{L_{osc}C'_{osc}}} \approx \frac{1}{2\pi\sqrt{L_{osc}(C_{osc} + AC_{tag})}} \left. \vphantom{\frac{1}{2\pi\sqrt{L_{osc}C'_{osc}}}} \right\} \Rightarrow \frac{1}{f_{osc}^2} \approx a + b \cdot RH + c \cdot RH^2 \quad (5)$$

$$C_{tag} = C_0 + C_1RH + C_2RH^2$$

where  $A$ ,  $C_0$ ,  $C_1$ ,  $C_2$ ,  $a$  and  $b$  are parameters independent from RH. In Figure 7 such dependence has been experimentally checked with a good fitting confirming the approximation in Equation 3. Indeed, experimental results of the inverse of the squared resonance frequency present very similar trend as the response to RH would be directly measured in the IDE capacitor (Figure 7), with a linear behavior between 20 and 70% RH and a bigger slope at higher relative humidity. Therefore, two different ranges can be used to calculate sensitivity using a linear fit. The first up to 70% and the second one for humidity higher than 70%. In the range of low relative humidity, the found sensitivity was  $(-1.88 \pm 0.17)$  kHz/%, thus obtaining an uncertainty of 1.7 % (covering factor equal to 1). For higher humidity, the obtained sensitivity was  $(-7.0 \pm 0.9)$  kHz/% with an uncertainty of 0.5 %. If a unique fit is used in the whole range a quadratic polynomial curve provided a reasonable fitting in the 10 to 90% RH.

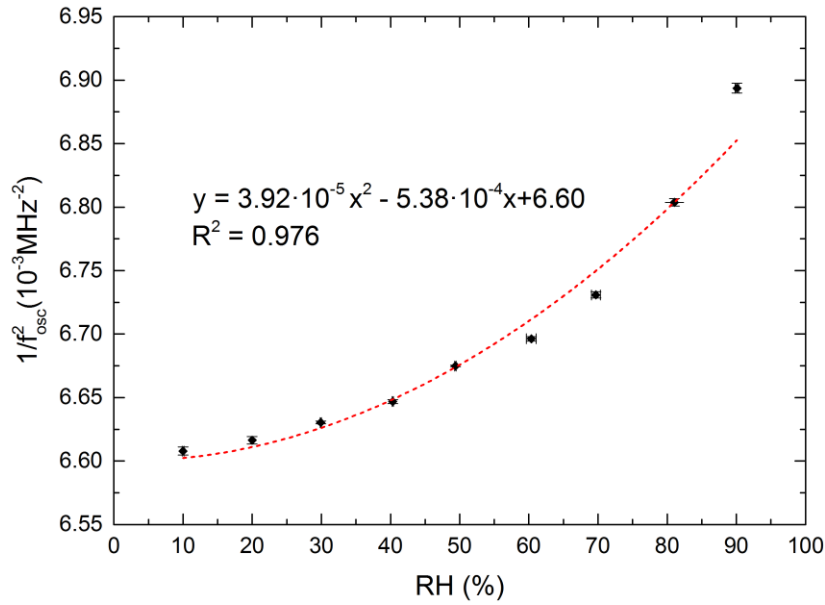


**Figure 7.** Inverse of the squared Colpitts oscillator frequency as a function of relative humidity.

## 6. Conclusions

A portable, low-cost, non-contact LC readout system for sensing-enabled HF tags has been developed and validated for humidity measurements using a fully printed passive chipless tag. The readout technique of the system is based on the change in the oscillation frequency of a Colpitts circuit when the LC tag is inductively coupled to the oscillator coil. This novel strategy avoids the need for high-cost and bulky equipment such as Impedance Analyzers or VNAs. Therefore, the system enables the use of chipless tags that can be deployed using mass production techniques compatible with industrial processes. To validate the reader for humidity sensing applications, a HF tag based on a parallel LC resonator structure was directly printed on a humidity-sensitive substrate. A significant change of about 260 kHz in the resonance frequency of the Colpitts circuit has been observed when relative humidity is varied from 10% to 90%. In the range of relative humidity lower than 70% the found sensitivity was  $(-1.88 \pm 0.17)$  kHz/% and the uncertainty was 1.7 %. For higher relative humidity the obtained sensitivity was  $(-7.0 \pm 0.9)$  kHz/% with an uncertainty of 0.5 %. Considering the flexible nature of the printed tag along with the reduced dimensions, compact design the reader, this system can be used for humidity monitoring in smart packaging applications.

## Acknowledgements

This work was supported by project CTQ2016-78754-C2-1-R from the Spanish Ministry of Economics and Competitivity. P. Escobedo wants to thank the Spanish Ministry of Education, Culture and Sport (MECD) for a pre-doctoral grant (FPU13/05032).

## References

- [1] K.B. Biji, C.N. Ravishankar, C.O. Mohan, T.K. Srinivasa Gopal, Smart packaging systems for food applications: a review, *J. Food Sci. Technol.* 52 (2015) 6125–6135. doi:10.1007/s13197-015-1766-7.
- [2] N. Zadbuke, S. Shahi, B. Gulecha, A. Padalkar, M. Thube, Recent trends and future of pharmaceutical packaging technology, *J. Pharm. Bioallied Sci.* 5 (2013) 98. doi:10.4103/0975-7406.111820.
- [3] M. Vanderroost, P. Ragaert, F. Devlieghere, B. De Meulenaer, Intelligent food packaging: The next generation, *Trends Food Sci. Technol.* 39 (2014) 47–62. doi:10.1016/j.tifs.2014.06.009.
- [4] E. Tan, W. Ng, R. Shao, B. Pereles, K. Ong, A Wireless, Passive Sensor for Quantifying Packaged Food Quality, *Sensors*. 7 (2007) 1747–1756. doi:10.3390/s7091747.
- [5] A. Nopwinyuwong, S. Trevanich, P. Suppakul, Development of a novel colorimetric indicator label for monitoring freshness of intermediate-moisture dessert spoilage, *Talanta*. 81 (2010) 1126–1132. doi:10.1016/j.talanta.2010.02.008.
- [6] R.A. Potyrailo, N. Nagraj, Z. Tang, F.J. Mondello, C. Surman, W. Morris, Battery-free Radio Frequency Identification (RFID) Sensors for Food Quality and Safety, *J. Agric. Food Chem.* 60 (2012) 8535–8543. doi:10.1021/jf302416y.
- [7] T. Unander, H.-E. Nilsson, Characterization of Printed Moisture Sensors in Packaging Surveillance Applications, *IEEE Sens. J.* 9 (2009) 922–928. doi:10.1109/JSEN.2009.2024866.
- [8] G. Stojanović, M. Radovanović, M. Malešev, V. Radonjanin, Monitoring of Water Content in Building Materials Using a Wireless Passive Sensor, *Sensors*. 10 (2010) 4270–4280. doi:10.3390/s100504270.
- [9] N. Barroca, L.M. Borges, F.J. Velez, F. Monteiro, M. Górski, J. Castro-Gomes, Wireless sensor networks for temperature and humidity monitoring within concrete structures, *Constr. Build. Mater.* 40 (2013) 1156–1166. doi:10.1016/j.conbuildmat.2012.11.087.
- [10] Q.-A. Huang, L. Dong, L.-F. Wang, LC Passive Wireless Sensors Toward a Wireless Sensing Platform: Status, Prospects, and Challenges, *J. Microelectromechanical Syst.* 25 (2016) 822–841. doi:10.1109/JMEMS.2016.2602298.
- [11] C. Li, Q. Tan, P. Jia, W. Zhang, J. Liu, C. Xue, et al., Review of Research Status and Development Trends of Wireless Passive LC Resonant Sensors for Harsh Environments, *Sensors*. 15 (2015) 13097–13109. doi:10.3390/s150613097.
- [12] K. Bao, D. Chen, Q. Shi, L. Liu, J. Chen, J. Li, et al., A readout circuit for wireless passive LC sensors and its application for gastrointestinal monitoring, *Meas. Sci. Technol.* 25 (2014) 085104. doi:10.1088/0957-0233/25/8/085104.
- [13] R. Nopper, R. Has, L. Reindl, A Wireless Sensor Readout System—Circuit Concept, Simulation, and Accuracy, *IEEE Trans. Instrum. Meas.* 60 (2011) 2976–2983. doi:10.1109/TIM.2011.2122110.
- [14] H. Farahani, R. Wagiran, M. Hamidon, Humidity Sensors Principle, Mechanism, and

- Fabrication Technologies: A Comprehensive Review, *Sensors*. 14 (2014) 7881–7939. doi:10.3390/s140507881.
- [15] E. Starke, A. Turke, M. Krause, W.-J. Fischer, Flexible polymer humidity sensor fabricated by inkjet printing, in: 2011 16th Int. Solid-State Sensors, Actuators Microsystems Conf., IEEE, 2011: pp. 1152–1155. doi:10.1109/TRANSDUCERS.2011.5969254.
- [16] F. Molina-Lopez, D. Briand, N.F. de Rooij, All additive inkjet printed humidity sensors on plastic substrate, *Sensors Actuators B Chem.* 166–167 (2012) 212–222. doi:10.1016/j.snb.2012.02.042.
- [17] F. Molina-Lopez, D. Briand, N.F. de Rooij, Inkjet and microcontact printing of functional materials on foil for the fabrication of pixel-like capacitive vapor microsensors, *Org. Electron.* 16 (2015) 139–147. doi:10.1016/j.orgel.2014.10.041.
- [18] J. Fernandez-Salmeron, A. Rivadeneyra, M.A.C. Rodriguez, L.F. Capitan-Vallvey, A.J. Palma, HF RFID Tag as Humidity Sensor: Two Different Approaches, *IEEE Sens. J.* 15 (2015) 5726–5733. doi:10.1109/JSEN.2015.2447031.
- [19] C. Gaspar, J. Olkkonen, S. Passoja, M. Smolander, Paper as Active Layer in Inkjet-Printed Capacitive Humidity Sensors, *Sensors*. 17 (2017) 1464. doi:10.3390/s17071464.
- [20] Y. Feng, L. Xie, Q. Chen, L.-R. Zheng, Low-Cost Printed Chipless RFID Humidity Sensor Tag for Intelligent Packaging, *IEEE Sens. J.* 15 (2015) 3201–3208. doi:10.1109/JSEN.2014.2385154.
- [21] F. Güder, A. Ainla, J. Redston, B. Mosadegh, A. Glavan, T.J. Martin, et al., Paper-Based Electrical Respiration Sensor, *Angew. Chemie Int. Ed.* 55 (2016) 5727–5732. doi:10.1002/anie.201511805.
- [22] A. Rivadeneyra, J. Fernández-Salmerón, M. Agudo-Acemel, J.A. López-Villanueva, L.F. Capitan-Vallvey, A.J. Palma, Printed electrodes structures as capacitive humidity sensors: A comparison, *Sensors Actuators, A Phys.* 244 (2016) 56–65. doi:10.1016/j.sna.2016.03.023.
- [23] F. Bibi, C. Guillaume, N. Gontard, B. Sorli, A review: RFID technology having sensing aptitudes for food industry and their contribution to tracking and monitoring of food products, *Trends Food Sci. Technol.* 62 (2017) 91–103. doi:10.1016/j.tifs.2017.01.013.
- [24] L. Catarinucci, R. Colella, L. Tarricone, A Cost-Effective UHF RFID Tag for Transmission of Generic Sensor Data in Wireless Sensor Networks, *IEEE Trans. Microw. Theory Tech.* 57 (2009) 1291–1296. doi:10.1109/TMTT.2009.2017296.
- [25] J. Virtanen, L. Ukkonen, T. Bjorninen, A.Z. Elsherbeni, L. Sydänheimo, Inkjet-Printed Humidity Sensor for Passive UHF RFID Systems, *IEEE Trans. Instrum. Meas.* 60 (2011) 2768–2777. doi:10.1109/TIM.2011.2130070.
- [26] R.A. Potyrailo, C. Surman, A passive radio-frequency identification (RFID) gas sensor with self-correction against fluctuations of ambient temperature, *Sensors Actuators B Chem.* 185 (2013) 587–593. doi:10.1016/j.snb.2013.04.107.
- [27] J. Gao, J. Siden, H.-E. Nilsson, M. Gulliksson, Printed Humidity Sensor With Memory Functionality for Passive RFID Tags, *IEEE Sens. J.* 13 (2013) 1824–1834. doi:10.1109/JSEN.2013.2244034.

- [28] J. Anum Satti, A. Habib, H. Anam, S. Zeb, Y. Amin, J. Loo, et al., Miniaturized humidity and temperature sensing RFID enabled tags, *Int. J. RF Microw. Comput. Eng.* 28 (2018) e21151. doi:10.1002/mmce.21151.
- [29] M. Mraović, T. Muck, M. Pivar, J. Trontelj, A. Pleteršek, Humidity Sensors Printed on Recycled Paper and Cardboard, *Sensors*. 14 (2014) 13628–13643. doi:10.3390/s140813628.
- [30] N. Javed, A. Habib, Y. Amin, J. Loo, A. Akram, H. Tenhunen, Directly printable moisture sensor tag for intelligent packaging, *IEEE Sens. J.* 16 (2016) 6147–6148. doi:10.1109/JSEN.2016.2582847.
- [31] A.W. Powell, D.M. Coles, R.A. Taylor, A.A.R. Watt, H.E. Assender, J.M. Smith, Plasmonic Gas Sensing Using Nanocube Patch Antennas, *Adv. Opt. Mater.* 4 (2016) 634–642. doi:10.1002/adom.201500602.
- [32] A.V. Quintero, F. Molina-Lopez, E.C.P. Smits, E. Danesh, J. van den Brand, K. Persaud, et al., Smart RFID label with a printed multisensor platform for environmental monitoring, *Flex. Print. Electron.* 1 (2016) 025003. doi:10.1088/2058-8585/1/2/025003.
- [33] J. Nie, J. Liu, N. Li, X. Meng, Dew point measurement using dual quartz crystal resonator sensor, *Sensors Actuators B Chem.* 246 (2017) 792–799. doi:10.1016/j.snb.2017.02.166.
- [34] V. Matko, D. Donlagic, Sensor for high-air-humidity measurement, *Sensors Actuators A Phys.* 61 (1997) 331–334. doi:10.1016/S0924-4247(97)01483-0.
- [35] R.G. Azevedo, W. Huang, O.M. O'Reilly, A.P. Pisano, Dual-mode temperature compensation for a comb-driven MEMS resonant strain gauge, *Sensors Actuators A Phys.* 144 (2008) 374–380. doi:10.1016/j.sna.2008.02.007.
- [36] V. Matko, Next Generation AT-Cut Quartz Crystal Sensing Devices, *Sensors*. 11 (2011) 4474–4482. doi:10.3390/s110504474.
- [37] A. Quddious, S. Yang, M. Khan, F. Tahir, A. Shamim, K. Salama, et al., Disposable, Paper-Based, Inkjet-Printed Humidity and H<sub>2</sub>S Gas Sensor for Passive Sensing Applications, *Sensors*. 16 (2016) 2073. doi:10.3390/s16122073.
- [38] X. Wang, O. Larsson, D. Platt, S. Nordlinder, I. Engquist, M. Berggren, et al., An all-printed wireless humidity sensor label, *Sensors Actuators B Chem.* 166–167 (2012) 556–561. doi:10.1016/j.snb.2012.03.009.
- [39] C. Zhang, L.-F. Wang, J.-Q. Huang, Q.-A. Huang, An LC-Type Passive Wireless Humidity Sensor System With Portable Telemetry Unit, *J. Microelectromechanical Syst.* 24 (2015) 575–581. doi:10.1109/JMEMS.2014.2333747.
- [40] J.H. Oum, S.E. Lee, D.-W. Kim, S. Hong, Non-contact heartbeat and respiration detector using capacitive sensor with Colpitts oscillator, *Electron. Lett.* 44 (2008) 87. doi:10.1049/el:20082336.
- [41] J. Luis, L. Roa Romero, J. Gómez-Galán, D. Hernández, M. Estudillo-Valderrama, G. Barbarov-Rostán, et al., Design and Implementation of a Smart Sensor for Respiratory Rate Monitoring, *Sensors*. 14 (2014) 3019–3032. doi:10.3390/s140203019.
- [42] D. Teichmann, J. Foussier, Jing Jia, S. Leonhardt, M. Walter, Noncontact Monitoring of Cardiorespiratory Activity by Electromagnetic Coupling, *IEEE Trans. Biomed. Eng.* 60

(2013) 2142–2152. doi:10.1109/TBME.2013.2248732.

- [43] D. Teichmann, D. De Matteis, T. Bartelt, M. Walter, S. Leonhardt, A Bendable and Wearable Cardiorespiratory Monitoring Device Fusing Two Noncontact Sensor Principles, *IEEE J. Biomed. Heal. Informatics.* 19 (2015) 784–793. doi:10.1109/JBHI.2015.2417760.
- [44] S. Vismantaitė, K. Kiniulytė, J. Grabauskaitė, M. Jucevičius, Capacitive Sensor for Respiratory Monitoring, (2016) 137–142.
- [45] N. Jeranče, N. Bednar, G. Stojanović, An Ink-Jet Printed Eddy Current Position Sensor, *Sensors.* 13 (2013) 5205–5219. doi:10.3390/s130405205.
- [46] T. Salpavaara, M. Järveläinen, S. Seppälä, T. Yli-Hallila, J. Verho, M. Vilkkko, et al., Passive resonance sensor based method for monitoring particle suspensions, *Sensors Actuators, B Chem.* 219 (2015) 324–330. doi:10.1016/j.snb.2015.04.121.
- [47] Y. Peng, T. Wang, W. Jiang, X. Liu, X. Wen, G. Wang, Modeling and Optimization of Inductively Coupled Wireless Bio-Pressure Sensor System Using the Design of Experiments Method, *IEEE Trans. Components, Packag. Manuf. Technol.* 8 (2018) 65–72. doi:10.1109/TCPMT.2017.2747138.
- [48] J. Coosemans, M. Catrysse, R. Puers, A readout circuit for an intra-ocular pressure sensor, *Sensors Actuators A Phys.* 110 (2004) 432–438. doi:10.1016/j.sna.2003.09.015.
- [49] A. Babu, B. George, A Linear and High Sensitive Interfacing Scheme for Wireless Passive LC Sensors, *IEEE Sens. J.* 16 (2016) 1–1. doi:10.1109/JSEN.2016.2614816.
- [50] H.L. Krauss, C.W. Bostian, F.H. Raab, *Solid State Radio Engineering*, John Wiley & Sons, Inc., Canada, 1980.
- [51] Daniel W.Hart, DC Power Supplies, in: *Power Electron.*, McGraw Hill, 2011: p. 266.
- [52] H.C. Luong, J. Yin, Transformer Design and Characterization in CMOS Process, in: *Transform. Des. Tech. Oscil. Freq. Divid.*, Springer International Publishing, Cham, 2016: pp. 7–19. doi:10.1007/978-3-319-15874-7\_2.
- [53] Dupont, DuPont™ Kapton® Summary of properties, (n.d.). <http://www.dupont.com/content/dam/dupont/products-and-services/membranes-and-films/polyimide-films/documents/DEC-Kapton-summary-of-properties.pdf>.
- [54] L. Gu, Q.-A. Huang, M. Qin, A novel capacitive-type humidity sensor using CMOS fabrication technology, *Sensors Actuators B Chem.* 99 (2004) 491–498. doi:10.1016/j.snb.2003.12.060.
- [55] A. Oprea, N. Barsan, U. Weimar, M.-L. Bauersfeld, D. Ebling, J. Wollenstein, Capacitive Humidity Sensors on Flexible RFID Labels, in: *TRANSDUCERS 2007 - 2007 Int. Solid-State Sensors, Actuators Microsystems Conf.*, IEEE, 2007: pp. 2039–2042. doi:10.1109/SENSOR.2007.4300564.
- [56] A. Rivadeneyra, J. Fernández-Salmerón, J. Banqueri, J. a. López-Villanueva, L.F. Capitan-Vallvey, A.J. Palma, A novel electrode structure compared with interdigitated electrodes as capacitive sensor, *Sensors Actuators B Chem.* 204 (2014) 552–560. doi:10.1016/j.snb.2014.08.010.